Neuroscience Research xxx (xxxx) xxx–xxx

Contents lists available at ScienceDirect

Neuroscience Research

journal homepage: www.elsevier.com/locate/neures

A mouse model of microglia-specific ablation in the embryonic central nervous system

Chenmin Li[a], Hiroyuki Konishi[a,*], Kimitoshi Nishiwaki[b], Katsuaki Sato[c], Takaki Miyata[d], Hiroshi Kiyama[a,*]

[a] Department of Functional Anatomy and Neuroscience, Nagoya University Graduate School of Medicine, Nagoya, 466-8550, Japan
[b] Department of Anesthesiology, Nagoya University Graduate School of Medicine, Nagoya, 466-8550, Japan
[c] Division of Immunology, Department of Infectious Diseases, Faculty of Medicine, University of Miyazaki, Kiyotake, Miyazaki, 889-1692, Japan
[d] Department of Anatomy and Cell Biology, Nagoya University Graduate School of Medicine, Nagoya, 466-8550, Japan

ARTICLE INFO

Article history:
Received 13 May 2021
Received in revised form 13 June 2021
Accepted 16 June 2021
Available online xxx

Keywords:
Embryo
Depletion
Development
Diphtheria toxin
In utero
Macrophage

ABSTRACT

Microglia, which migrate into the central nervous system (CNS) during the early embryonic stages, are considered to play various roles in CNS development. However, their embryonic roles are largely unknown, partly due to the lack of an effective microglial ablation system in the embryo. Here, we show a microglial ablation model by injecting diphtheria toxin (DT) into the amniotic fluid of *Siglech*^{dtr} mice, in which the gene encoding DT receptor is knocked into the microglia-specific gene locus *Siglech*. We revealed that embryonic microglia were depleted for several days throughout the CNS, including some regions where microglia transiently accumulated, at any embryonic time point from embryonic day 10.5, when microglia colonize the CNS. This ablation system was specific for microglia because CNS-associated macrophages, which are a distinct population from microglia that reside in the CNS interfaces such as meninges, were unaffected. Therefore, this microglial ablation system is highly effective for studying the embryonic functions of microglia.

1. Introduction

Microglia, a type of mononuclear cells in the central nervous system (CNS), solely originate from embryonic macrophage precursors in the yolk sac and invade the brain at embryonic day (E) 9.5–10.5 (Ginhoux et al., 2010; Kierdorf et al., 2013; Hoeffel et al., 2015; Ginhoux and Guilliams, 2016). Given colonizing the CNS prior to the generation of neurons, astrocytes, and oligodendrocytes (Silva et al., 2019), microglia are thought to participate in various CNS developmental events. Recent studies have revealed some microglial functions during postnatal development, such as neuronal survival and elimination (Marín-Teva et al., 2004; Ueno et al., 2013), synapse formation and elimination (Paolicelli et al., 2011; Schafer et al., 2012; Miyamoto et al., 2016), and myelin formation (Wlodarczyk et al., 2017). In contrast, microglial function in the embryonic CNS remains poorly understood. Several studies have shown that microglia play a role in neurogenesis (Cunningham et al., 2013), neuronal differentiation (Hattori and Miyata, 2018; Hattori et al., 2020), and axonal elongation (Squarzoni et al., 2014). However, studies reporting functions of microglia during the embryonic period are significantly fewer than those during postnatal development.

A microglia-specific ablation system is a useful tool in investigating the novel functions of microglia. In addition to parenchymal microglia, several types of macrophages reside in CNS interfaces, such as perivascular spaces, leptomeninges, and choroid plexus in adult mice (Goldmann et al., 2016; Prinz et al., 2017). Given that these CNS-associated macrophages (CAMs) are mostly of embryonic origin and colonize CNS interfaces during the embryonic stage like microglia (Goldmann et al., 2016; Utz et al., 2020), embryonic microglial ablation systems for studying their functions are required to minimize damage to CAMs.

Various types of microglial ablation methods have been reported in adult mice. Pharmacologically, the CSF-1R inhibitor PLX3397 or PLX5622, which significantly inhibits the survival signal of microglia, has been used frequently because oral administration

Abbreviations: CAMs, CNS-associated macrophages; CC, corpus callosum; CNS, central nervous system; CP, cortical plate; DAPI, 4′,6-diamidono-2-phenylindole; DREZ, dorsal root entry zone; DT, diphtheria toxin; DTA, DT fragment A; DTR, DT receptor; E, embryonic day; IZ/SVZ/VZ, intermediate zone/subventricular zone/ventricular zone; PBS, phosphate buffered saline; WT, wild-type.

* Corresponding authors at: Department of Functional Anatomy and Neuroscience, 65, Tsurumai-cho, Showa-ku, Nagoya, 466-8550, Japan.
E-mail addresses: konishi@med.nagoya-u.ac.jp (H. Konishi), kiyama@med.nagoya-u.ac.jp (H. Kiyama).

https://doi.org/10.1016/j.neures.2021.06.002
0168-0102/

of the chow containing these reagents can conveniently deplete almost all microglia in adult mice (Elmore et al., 2014). However, these PLX compounds are also effective for various types of peripheral macrophages and CAMs (Van Hove et al., 2019; Lei et al., 2020). Indeed, PLX5622 eliminates more than 99% of microglia in embryonic mice when the reagent is administered to dams; however, embryonic exposure to PLX5622 causes craniofacial and dental abnormalities, possibly due to impaired functions of peripheral macrophages and/or osteoclasts (Rosin et al., 2018), suggesting that PLX5622 also depletes CAMs in the embryonic brain. In addition to pharmacological strategies, mice deficient in *Sfpi1* (gene encoding PU.1) or *Csf1r* are used because these mutant mice are devoid of microglia (Erblich et al., 2011; Squarzoni et al., 2014). However, embryonic macrophages are also affected in these mice, although the extent to which they are affected depends on the type of CAM (Angelim et al., 2018; Munro et al., 2020). For conditional ablation of microglia in adulthood, microglia- or mononuclear lineage-specific CreER driver mice are crossed with Cre-inducible "diphtheria toxin (DT) receptor (DTR)" or "DT fragment A (DTA)," or $Csf1r^{fl/fl}$ mice (Cronk et al., 2018; Han et al., 2019). The most commonly used CreER driver line is $Cx3Cr1^{CreER}$ (Yona et al., 2013). However, the $Cx3Cr1^{CreER}$-based system is very likely to ablate CAMs in addition to microglia in embryonic mice, given that CX3CR1 is also expressed by embryonic CAMs (Goldmann et al., 2016). To improve the specificity of microglia, several CreER driver lines, $Sall1^{CreER}$ (Buttgereit et al., 2016), $Tmem119^{CreER}$ (Kaiser and Feng, 2019), $P2ry12^{CreER}$ (McKinsey et al., 2020), and $Hexb^{CreER}$ (Masuda et al., 2020), all of which use gene loci highly specific to microglia in adulthood, have been reported recently. Among these CreER driver lines, at least $P2ry12^{CreER}$ could achieve specific ablation of microglia in the embryo, given the specificity and expression level of P2Y12 in embryonic microglia (Mildner et al., 2017). However, tamoxifen treatment of pregnant mice is known to have adverse effects on their embryos (Rojo et al., 2018; Ved et al., 2019; Lee et al., 2020). Particularly, Lee et al. (Lee et al., 2020) recently demonstrated, using single-cell RNA sequencing, that embryonic exposure to tamoxifen dysregulates Wnt signaling to impair neurogenesis and cortical organization. Therefore, a CreER-dependent system would not be suitable.

Here, we present a new model of embryonic microglial ablation with high efficiency and specificity. Our previous study reported that Siglec-H is a microglia-specific marker that is almost negative for CAMs (Konishi et al., 2017). Accordingly, systemic administration of DT to $Siglech^{dtr/dtr}$ mice, in which the gene encoding DTR was knocked into the *Siglech* locus, achieved specific ablation of microglia on postnatal day 7 or after (Konishi et al., 2017, 2020). Given that the microglia-specific expression of Siglec-H was observed at the later embryonic stage in our previous study (Konishi et al., 2017), we expected that this ablation system would be applicable to embryos. In this study, we mated $Siglech^{dtr/dtr}$ mice with wild-type (WT) mice to generate $Siglech^{dtr/+}$ embryos, in which we examined microglial ablation by DT injection into the amniotic fluid. Our results demonstrated that microglia were depleted for several days after DT injection without influencing CAMs. Microglia-specific ablation is effective at any time point from E10.5, when colonized microglia start to expand broadly throughout the CNS (Ginhoux et al., 2010), indicating the significance of this ablation system for studying the embryonic functions of microglia.

2. Materials and methods

2.1. Animals

All experiments were conducted according to the guidelines of the Animal Ethics Committees of the Nagoya University Graduate School of Medicine, the Animal Protection and Management Law of Japan (No. 105), and the 3R principle (replacement, refinement, and reduction). C57BL/6 WT mice were purchased from Charles River Laboratories Japan. $Siglech^{dtr}$ mice (B6.Cg-$Siglech^{<tm1.1Ksat>}$ mice; deposited in the RIKEN BioResource Center [accession number: RBRC05658]) were described previously (Takagi et al., 2011). To generate heterozygous $Siglech^{dtr/+}$ embryos, we crossed $Siglech^{dtr/dtr}$ male mice (older than 8-week-old [W]) with WT female mice (8–12 W). All animal experiments were performed under the condition of a reversed 12 h light/dark cycle with free access to food and water.

2.2. In utero injection of DT

A plug check was conducted in the morning, and the day when a vaginal plug was detected was regarded as E0.5. $Siglech^{dtr/+}$ embryos at E10.5, 12.5, 14.5, and 16.5 were used. The injection method was established based on our previous study on *in utero* electroporation (Saito et al., 2019). Pregnant mice were anesthetized with isoflurane, and an abdominal incision was made. The uterus was then exposed onto gauze moistened with phosphate buffered saline (PBS). With illuminating embryos in the uterus by a flexible light source (Hoya-schott), DT (20 ng/μl) diluted with PBS containing 0.3% non-toxic dye Fast Green was injected into amniotic fluid using glass micropipettes. The volume of DT solution was determined depending on the weight of embryos: 2, 5, 8, and 11 μl for E10.5, 12.5, 14.5, and 16.5, respectively (DT dose: approximately 280 ng/embryonic weight [g]). In the control group, the same volume of PBS was injected.

2.3. Tissue fixation for immunohistochemistry

The pregnant mice were deeply anesthetized, and embryos were dissected from the uterus at E10.5, 12.5, E14.5, E16.5, and E18.5. Embryos at E10.5, 12.5, and E14.5 were entirely fixed in Zamboni's fixative (0.1 M phosphate buffer containing 2% paraformaldehyde and 0.2% picric acid) for 6 h at 4 °C. For embryos at E16.5 and E18.5, to avoid the delayed fixation of neural tissues due to the larger body size, brains and spines were dissected from the embryos, and then fixed in Zamboni's fixative for 6 h at 4 °C.

2.4. Immunohistochemistry for sections

Fixed embryos, brains, and spines were dehydrated in 25% sucrose with 0.1 M phosphate buffer overnight at 4 °C and frozen with dry ice. Coronal sections (16 μm thickness) were prepared using a cryostat (CM1950, Leica) and washed with 0.01 M PBS. After blocking and permeabilization for 30 min in blocking solution (0.01 M PBS containing 0.5% bovine serum albumin, 0.1% TritonX-100, and 0.1% NaN_3), the sections were incubated with primary antibodies diluted in blocking solution overnight at 4 °C. After washing with 0.01 M PBS, sections were subsequently incubated with secondary antibodies diluted in 0.01 M PBS at room temperature for 2 h. 4′,6-diamidono-2-phenylindole (DAPI) staining was performed as necessary. After immunostaining was completed, the sections were mounted with FluorSave reagent (Merck Millipore). The following primary antibodies were used: goat polyclonal anti-Iba-1 (Abcam #ab5076, RRID: AB_2224402; 1:1000), rabbit polyclonal anti-CD206 (Abcam #ab64693, RRID: AB_1523910; 1:1000), rat monoclonal anti-CD206 (Bio-Rad #MCA2235GA, RRID: AB_322631; 1:500), rabbit polyclonal anti-P2Y12 (AnaSpec #AS-55043A, RRID: AB_2298886; 1:500), and sheep anti-Siglec-H (Zhang et al., 2006). Secondary antibodies conjugated with Alexa Fluor 488, 594, and 647 were used (Thermo Fisher Scientific or Abcam; 1:1000). Fluo-

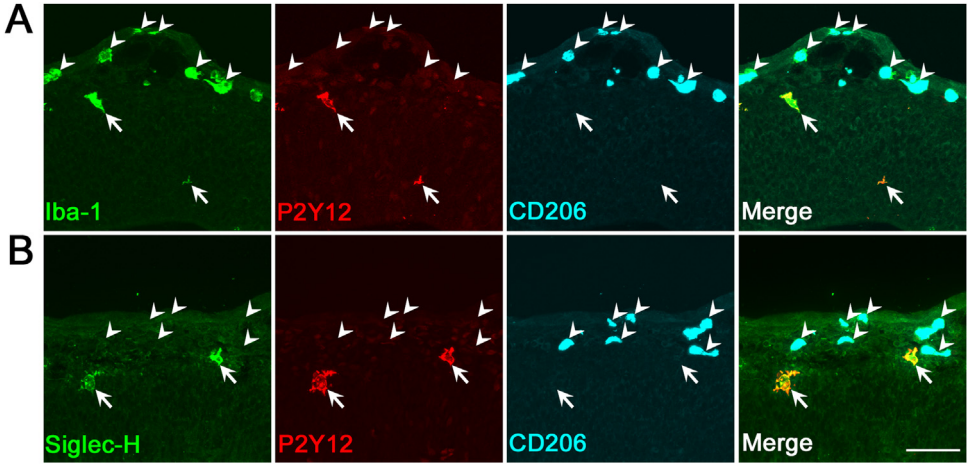

Fig. 1. Siglec-H is specifically expressed by microglia in the embryonic CNS. A. Cerebral cortex immunostained with Iba-1 (green), P2Y12 (red), and CD206 (cyan) at E12.5. Iba-1$^+$P2Y12$^+$ microglia in the cortical parenchyma (arrows); Iba-1$^+$CD206$^+$ meningeal macrophages in cortical surfaces (arrowheads). B. Cerebral cortex immunostained with Siglec-H (green), P2Y12 (red), and CD206 (cyan). Siglec-H$^+$P2Y12$^+$ microglia in cortical parenchyma (arrows); Siglec-H$^-$CD206$^+$ meningeal macrophages in cortical surfaces (arrowheads). Scale bar =50 μm.

rescent images were visualized using an FV10i confocal microscope (Olympus).

2.5. Whole-mount immunohistochemistry of spinal cords

Spinal cords were dissected from embryos at E12.5. The staining method was the same as for the sections except for the reaction durations: blocking (3 h) and secondary antibody (10 h). After staining, spinal cords were mounted onto glass slides as open-book preparations with FluorSave reagent and imaged using an FV10i confocal microscope.

2.6. Statistical analyses

We defined parenchymal Iba-1$^+$CD206$^-$ cells and meningeal Iba-1$^+$CD206$^+$ cells as microglia and macrophages, respectively. The numbers of microglia and meningeal macrophages were normalized to the area and length of the outer circumference of tissues, respectively. To minimize inter-individual differences, DT-injected embryos (2–4 embryos/dam) were compared with their littermates with PBS injection (2–4 embryos/dam) in the same dam. At least four images (one field/section, 2–4 sections/embryo, and 2–4 embryos) were taken from one dam. A total of at least 16 images (four images/dam, four dams) were analyzed for each group. Values are represented as the mean ± SEM. Statistical significance was determined by the paired Student's *t*-test, and $p < 0.05$ was considered statistically significant.

3. Results

3.1. Siglec-H is specifically expressed by microglia in the embryonic CNS

Our previous study demonstrated that Siglec-H is specifically expressed by microglia in the CNS at late embryonic stages after E17.5 (Konishi et al., 2017). To verify Siglec-H specificity in earlier embryonic stages, we performed immunohistochemistry (Fig. 1). In the cerebral cortex of WT mice at E12.5, when both microglia and CAMs were already present in the CNS (Utz et al., 2020), we identified microglia by the expression of P2Y12, whose expression was reported to be confined to microglia even in embryos (Mildner et al., 2017; Utz et al., 2020) (Fig. 1A). In addition to microglia, we found many CD206$^+$ meningeal macrophages on cortical surfaces, while brain parenchyma contained few CD206$^+$ perivascular macrophages, as described previously (Galea et al., 2005; Utz et al., 2020). In contrast to the cell-type-specific expression of P2Y12 and CD206 in microglia and meningeal macrophages, respectively, Iba-1 was expressed in both cell types, which is in line with a previous report (Utz et al., 2020). When we stained the sections with Siglec-H antibody, Siglec-H expression was observed in P2Y12$^+$ microglia, but not in other cell types including CD206$^+$ macrophages (Fig. 1B), demonstrating the marker specificity of Siglec-H in embryonic mice. We obtained consistent results in other regions of the CNS, including the hippocampus and spinal cord (data not shown). Thus, both Siglec-H and P2Y12 are reliable immunohistochemical markers of embryonic microglia. However, the shapes of some microglia could not be visualized clearly by either Siglec-H or P2Y12 immunostaining, probably because both molecules are membrane proteins. Therefore, in this study, we used neither Siglec-H nor P2Y12 for microglial identification. Instead, we performed double-immunostaining of Iba-1 and CD206 and defined Iba-1$^+$CD206$^-$ cells and Iba-1$^+$CD206$^+$ cells as microglia and meningeal macrophages, respectively.

3.2. Microglia can be depleted for 4 days after a single injection of DT at E10.5 in utero

Our previous studies demonstrated that microglia were able to be ablated by the systemic administration of DT in adult *Siglech*$^{dtr/+}$ or *Siglech*$^{dtr/dtr}$ mice (Konishi et al., 2017, 2020). We first tested microglial ablation by the administration of DT at E10.5, when few Iba-1$^+$CD206$^-$ microglia were already seen in the brain (data not shown). We crossed *Siglech*$^{dtr/dtr}$ male mice with WT female mice to generate *Siglech*$^{dtr/+}$ embryos. Because intraperitoneal injection of DT into dams was not able to ablate microglia in their embryos in our preliminary experiment, we injected DT into the amniotic fluid of *Siglech*$^{dtr/+}$ embryos at E10.5 on the hypothesis that DT infused into the amniotic fluid might be transported to the CNS (Fig. 2A). Brain sections at E12.5 demonstrated that the microglial number in the cerebral cortex was significantly lower in the DT group than in the PBS control group, while the number of meningeal CD206$^+$ macrophages remained unchanged (Fig. 2B). Next, to investigate the duration of microglial depletion, we assessed brain sections at E14.5, 16.5, and 18.5, revealing that microglial depletion was sustained until E14.5 in DT groups. Quantitative studies indicated that microglial numbers in DT groups were decreased to 21.8% and

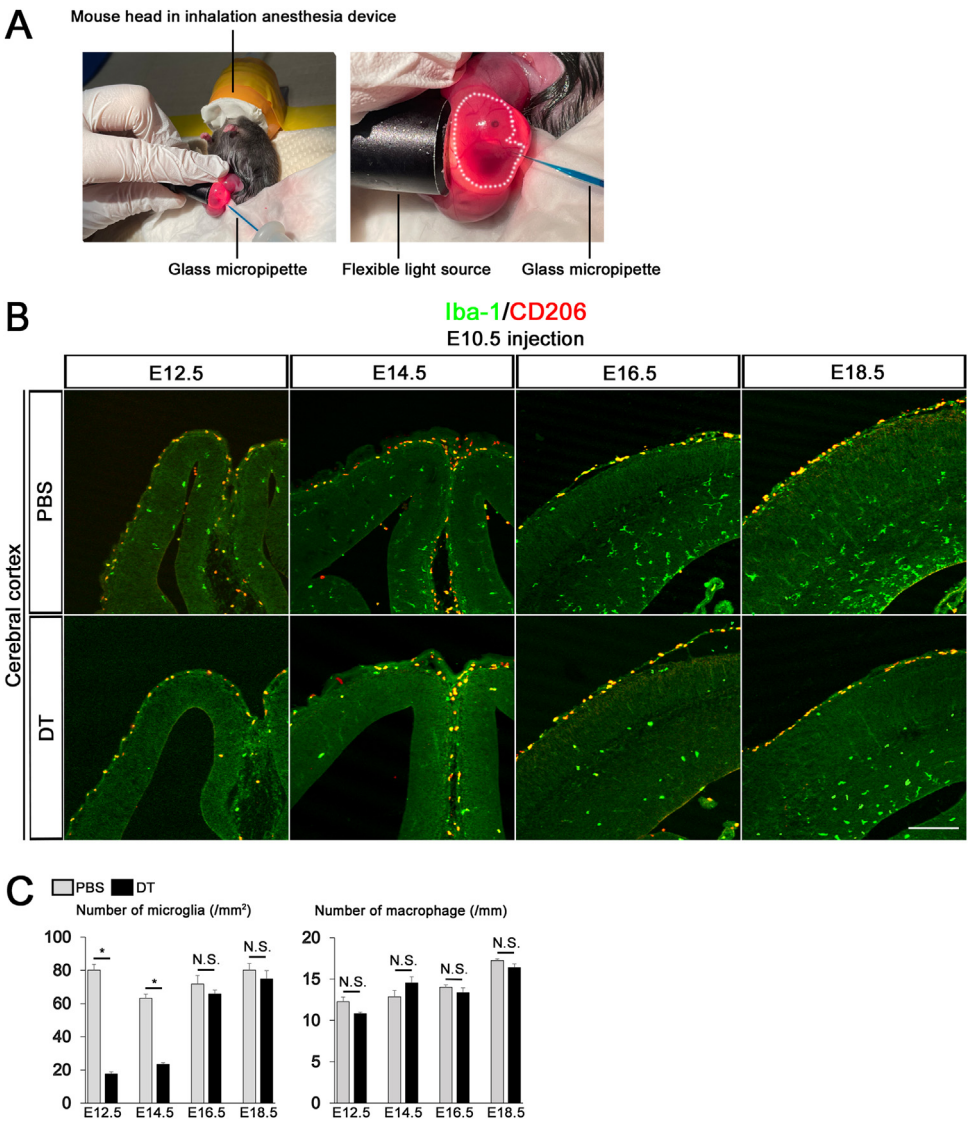

Fig. 2. Microglia-specific ablation in the cerebral cortex with the injection of DT at E10.5. A. Images showing the injection method. Note that E14.5, not E10.5, embryos are used for this image to clearly show the embryonic shape in the uterus. B. Cerebral cortex immunostained with Iba-1 (green) and CD206 (red) at E12.5, 14.5, 16.5, and 18.5 after the injection of PBS or DT *in utero* at E10.5. Scale bar =200 μm. C. Quantification of the number of Iba-1$^+$CD206$^-$ microglia (per parenchymal area) and Iba-1$^+$CD206$^+$ macrophages (per the length of the surface of the cerebral cortex) at E12.5, E14.5, E16.5, and E18.5. Statistical significance was determined by the paired Student's *t*-test. N.S.: no significance; $^*p < 0.001$.

36.5% at E12.5 and 14.5, respectively, and then returned to the control level at E16.5 and E18.5 (Fig. 2C). In contrast, there was no significant difference in the number of Iba-1$^+$CD206$^+$ meningeal macrophages between the PBS and DT groups at any time point (Fig. 2C).

In addition to the forebrain, we also examined spinal cord sections and obtained consistent results (Fig. 3A and B). When DT was injected at E10.5, the microglial number significantly decreased at E12.5, E14.5 and then returned to the control level at E16.5 and E18.5. There were no differences in the number of meningeal macrophages between the PBS and DT groups at any time point. Previous studies reported that microglia accumulated in the dorsolateral region of the spinal cord at E12.5 (Rigato et al., 2011; Angelim et al., 2018). Spinal cord sections at E12.5 demonstrated that the accumulated microglia in the dorsolateral region, presumably the dorsal root entry zone (DREZ), where the dorsal root enters the spinal dorsal horn, were also ablated by DT injection (arrows in Fig. 3A). To clearly demonstrate this result, we further examined whole-mount immunostaining of spinal cords at E12.5 (Fig. 3C). Accumulated microglia appeared as longitudinal bundles at both sides of the spinal cord in the PBS groups. However, bundle-like microglial accumulation almost disappeared in the DT groups, although CD206$^+$ macrophages remained. These results indicate that with the *in utero* injection of DT at E10.5, microglia could be eliminated for almost 4 days without affecting the number of meningeal macrophages.

3.3. *Microglia can be ablated at any embryonic time point after E10.5*

To test whether this microglial ablation model was also effective at later embryonic stages, we changed the injection time points. We injected DT at E12.5, E14.5, or E16.5 and analyzed the embryos after 2 days. Regardless of the injection time points, microglia were ablated 2 days after DT injection in the cerebral cortex, although meningeal macrophages were not affected (Fig. 4A and B). Previous studies have shown that microglia accumulate in the intermediate zone/subventricular zone/ventricular zone (IZ/SVZ/VZ) of the

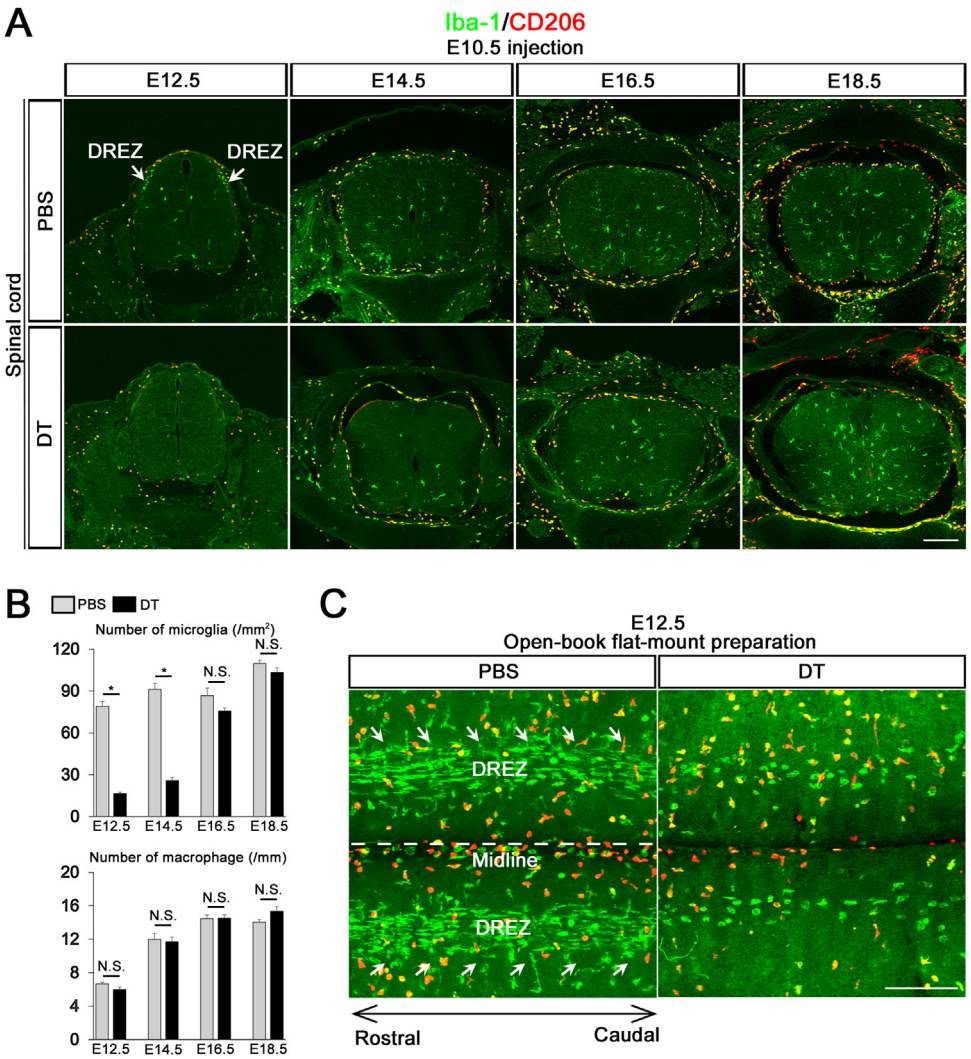

Fig. 3. Microglia-specific ablation in the spinal cord with the injection of DT at E10.5. A. Spinal cord immunostained with Iba-1 (green) and CD206 (red) at E12.5, 14.5, 16.5, and 18.5 after the injection of PBS or DT *in utero* at E10.5. Arrows indicate DREZ where microglia transiently accumulate in the PBS group at E12.5. Scale bar =200 μm. B. Quantification of the number of Iba-1$^+$CD206$^-$ microglia (per parenchymal area) and Iba-1$^+$CD206$^+$ macrophages (per the length of the outer circumference of the spinal cord) at E12.5, E14.5, E16.5, and E18.5. Statistical significance was determined by the paired Student's *t*-test. N.S.: no significance; $^*p < 0.001$. C. Open-book flat-mount samples of the spinal cord immunostained with Iba-1 and CD206 at E12.5 after the injection of PBS or DT at E10.5. The dotted line indicates the midline. Arrows delineate DREZ. Scale bar =200 μm.

cerebral cortex at E15.5–16.5, exerting some specific functions (Cunningham et al., 2013; Squarzoni et al., 2014; Hattori et al., 2020). As shown in these previous studies, microglia colonized the IZ/SVZ/VZ but were almost absent in the cortical plate (CP) in PBS groups at E16.5. DT injection at E14.5 significantly decreased the microglial number in IZ/SVZ/VZ at E16.5. Similar results were obtained in the spinal cord 2 days after injection at E12.5, E14.5, or E16.5 (Fig. 4C and D). In addition to the cerebral cortex and spinal cord, we examined the hippocampus (Fig. 4E and F). Although the hippocampal primordium already existed at E14.5 (Urbán and Guillemot, 2014), we did not analyze the hippocampi of E14.5 embryos injected with DT at E12.5 because of its small size. Injection of DT at E14.5 and E16.5 significantly decreased the number of microglia in the hippocampus after 2 days (Fig. 4E and F). Meningeal macrophages surrounding the hippocampus were not analyzed because the cells did not cover the entire circumference of the hippocampus (Fig. 4E).

At the later embryonic stage (around E17.5), the microglia that assembled at the midline region beneath the corpus callosum (CC) presumably regulated the fasciculation of the CC axon tract (Pont-Lezica et al., 2014). DT injection at E16.5 eliminated most of the accumulated microglia beneath CC at E18.5 (arrows in Fig. 4G), although there remained CD206$^+$ presumable macrophages beneath the CC (small arrowheads in Fig. 4G), whose characteristics were not determined further in the present study, and CD206$^+$ meningeal macrophages of the cingulate cortex (large arrowheads in Fig. 4G). Collectively, this ablation system can eliminate microglia throughout the CNS, including the specific regions where microglial density is transiently high, at any time point after microglial colonization in the CNS.

4. Discussion

Microglia originate solely from the yolk sac and invade the CNS at E9.5–10.5 (Ginhoux et al., 2010; Kierdorf et al., 2013; Hoeffel et al., 2015; Ginhoux and Guilliams, 2016). The embryonic functions of microglia remain poorly understood. Therefore, to study their functions, the establishment of a microglial ablation system in embryonic mice is expected. In this study, we applied our microglial ablation model, whose utility in postnatal mice was evaluated in our previous study (Konishi et al., 2017, 2020), to embryonic stages. We first confirmed that Siglec-H is specifically expressed

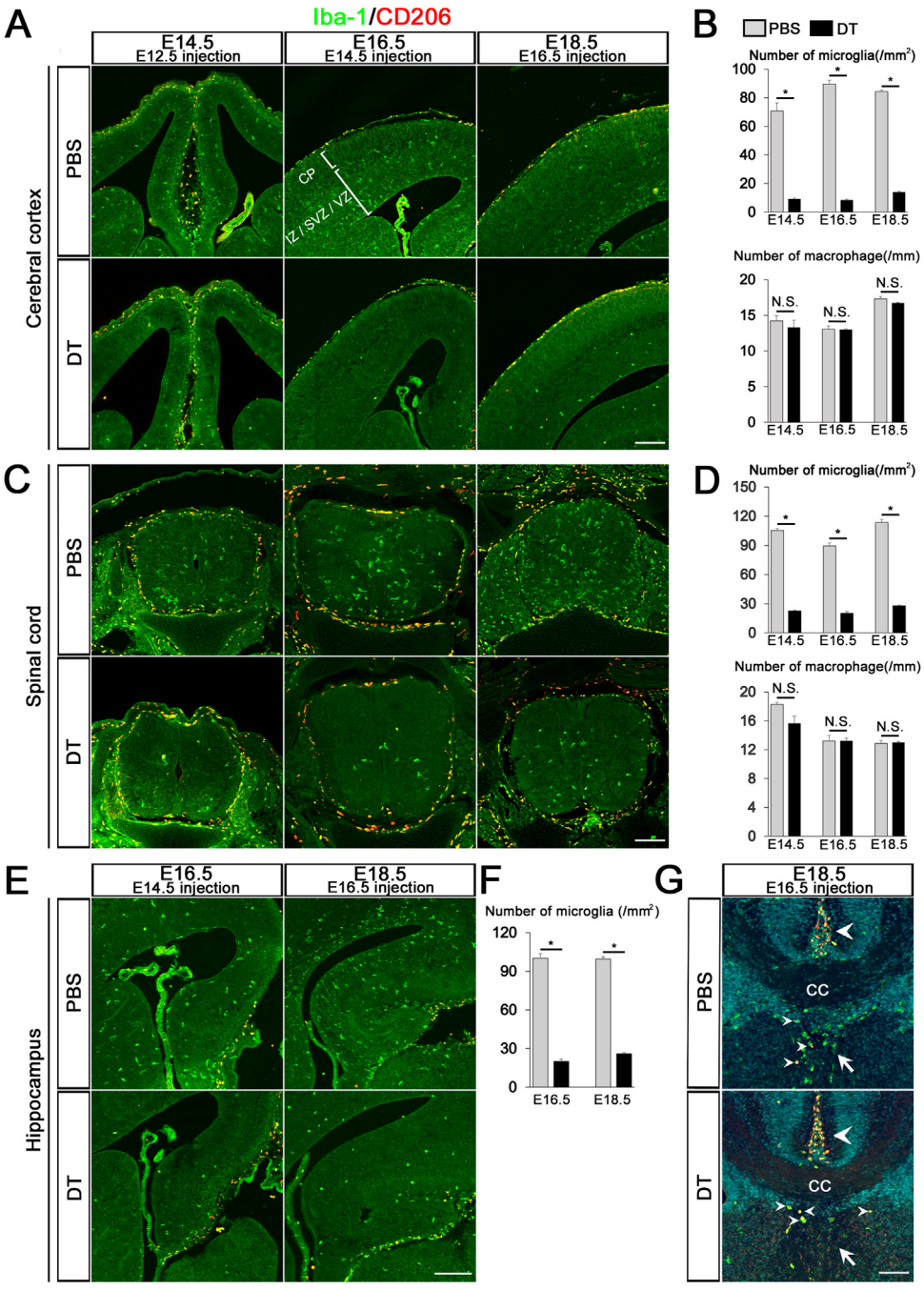

Fig. 4. Microglia-specific ablation in three representative regions of the CNS with the injection of DT at E12.5, 14.5, and 16.5. Sections of the cerebral cortex (A) and spinal cord (C) immunostained with Iba-1 (green) and CD206 (red) 2 days after the injection of PBS or DT at E12.5, E14.5, and E16.5. Note that microglia colonized the IZ/SVZ/VZ but were almost absent in the CP in PBS groups at E16.5. Hippocampal sections 2 days after the injection at E14.5 and E16.5 are also shown (E). Scale bar =200 μm (A, C, E). (B, D, F) Quantification of the number of Iba-1^{+}CD206^{-} microglia (per parenchymal area) and Iba-1^{+}CD206^{+} macrophages (per the length of the outer circumference of the tissue) in the cerebral cortex (B), spinal cord (D), and hippocampus (F). Statistical significance was determined by the paired Student's *t*-test. N.S.: no significance; $^{*}p < 0.001$. G. Images around CC stained with Iba-1 (green) and CD206 (red) antibodies, and DAPI (cyan) at E18.5 after the injection of PBS or DT at E16.5. Arrows indicate a region at the midline region beneath the CC, where microglial accumulation was observed in the PBS group. Small and large arrowheads indicate presumptive macrophages in the region beneath the CC and meningeal macrophages in the cingulate cortex, respectively. Scale bar =100 μm.

by parenchymal microglia but not by meningeal macrophages in embryonic mice (Fig. 1). We then demonstrated that microglia could be depleted throughout the CNS for several days by injecting DT into the amniotic fluid of *Siglech*$^{dtr/+}$ embryos, although meningeal macrophages were unaffected (Figs. 2–4). The ablation system was also effective for specific CNS regions, where microglia transiently accumulated presumably to play some roles. Furthermore, DT-treated embryos can be compared with their littermates treated with vehicle in the same dam, indicating the utility of this ablation system for studying the embryonic functions of microglia.

CD206^{+} CAMs emerge in the yolk sac like microglia and are clearly identified in the CNS, especially at the meninges, at E10.5. Therefore, for microglia-specific ablation using genetically engineered mice, the selection of gene loci or promoters is important. Several microglia-specific marker molecules whose expression is absent in most CAMs have been identified recently in adult mice, such as Hexb, P2Y12, Sall1, Siglec-H, and TMEM119 (Bennett et al.,

2016; Buttgereit et al., 2016; Konishi et al., 2017; Mildner et al., 2017; Masuda et al., 2020). However, some of these could not be microglial markers during the embryonic stage. For instance, TMEM119 expression is absent in immature microglia during embryonic stages (Bennett et al., 2016). Sall1 is also expressed by neuronal/glial progenitor cells (Harrison et al., 2012). In contrast, we demonstrated the specific expression of Siglec-H in microglia in the embryonic CNS (Fig. 1), similar to the adult CNS shown in our previous study (Konishi et al., 2017). We then examined the administration of DT to *Siglech*$^{dtr/+}$ embryos. For a cell ablation system using adult mice expressing DTR, systemic injection of DT is the standard method (Buch et al., 2005). However, intraperitoneal injection of DT into dams was not able to ablate microglia in their embryos in our preliminary experiment presumably because of the placental barrier that prevents the passage of most maternal proteins (Malek et al., 1998). Therefore, we injected DT into the amniotic fluid of *Siglech*$^{dtr/+}$ embryos *in utero*, demonstrating that a considerable number of microglia were ablated. A previous study, which established *P2ry12*^{CreER} mice, showed that robust recombination occurred specifically in microglia, even in embryonic mice (McKinsey et al., 2020). Thus, microglia-specific ablation is assumed to be achieved by maternal administration of tamoxifen to *P2ry12*^{CreER} mice crossed with Cre-dependent cell ablation lines such as *Rosa26*^{DTA} mice (Voehringer et al., 2008). However, tamoxifen has some artificial effects on the embryonic CNS, such as an increased number of macrophages and impaired neurogenesis (Rojo et al., 2018; Lee et al., 2020), suggesting that the employment of CreER driver mice would not be suitable for studying the embryonic functions of microglia.

Given the diverse functions of microglia during postnatal development (Marín-Teva et al., 2004; Paolicelli et al., 2011; Schafer et al., 2012; Ueno et al., 2013; Miyamoto et al., 2016; Wlodarczyk et al., 2017; Konishi et al., 2019), microglia are expected to play roles in some embryonic events in the CNS. Previous studies have found that embryonic microglia transiently accumulate in some regions, such as IZ/SVZ/VZ of the cerebral cortex (Fig. 4) (Cunningham et al., 2013; Squarzoni et al., 2014; Hattori et al., 2020), DREZ of the spinal cord (Fig. 3) (Rigato et al., 2011; Angelim et al., 2018), and the midline region beneath the CC (Fig. 4) (Pont-Lezica et al., 2014). Microglia are suggested to play specific roles in these "hot spots." Microglia phagocytose neural precursor cells to decrease the size of the precursor pool in the SVZ/VZ (Cunningham et al., 2013). In DREZ, microglia may secrete some factors that support the survival of dorsal root ganglion neurons (Angelim et al., 2018). Microglia around the CC promote fasciculation of callosal axons (Pont-Lezica et al., 2014). Although to a lesser extent than in these hot spots, microglial density is high along the wall of the third ventricle at E13.5–17.5, where microglia may regulate hypothalamic neurogenesis/gliogenesis (Rosin et al., 2018; Marsters et al., 2020). Some of these microglial functions have been suggested by the results of microglial ablation models with PLX5622 administration to dams (Rosin et al., 2018; Marsters et al., 2020), maternal inflammation model with lipopolysaccharide injection (Pont-Lezica et al., 2014), or microglia-free *Sfpi1*$^{-/-}$ mice (Pont-Lezica et al., 2014; Angelim et al., 2018). In these mouse models, however, CAMs are likely affected in addition to microglia, raising the possibility that the observed phenotypes might be derived from abnormalities in CAMs. In contrast, our ablation model discriminates this possibility, indicating its utility in future studies on embryonic microglia.

In conclusion, we have established a microglia-specific ablation model that is effective throughout the CNS at any time point of embryonic stages after microglial expansion to the CNS. Microglial dysregulation during the embryonic stage is thought to result in the abnormal formation of neural circuits, which eventually causes developmental brain disorders (Thion et al., 2018). To develop new therapeutic strategies, understanding microglial functions is necessary. Future studies using this ablation system may reveal novel or precise functions of embryonic microglia.

Declaration of Competing Interest

The authors report no declarations of interest.

Acknowledgments

This work was supported by KAKENHI ["Grant-in-Aid for Scientific Research (B)" 19H03395 to H. Kiyama, "Grant-in-Aid for Scientific Research (C)" 19K06904 to H. Konishi] from the Ministry of Education, Culture, Sports, Science and Technology (MEXT) of Japan, and by grants from the Nakatomi Foundation to H. Konishi. We are grateful to Dr. P. Crocker (University of Dundee) for the anti-Siglec-H antibody and Ms. N. Noguchi, A. Asano, Y. Itai, N. Tawarayama, and K. Muraki for technical assistance. We would like to thank Editage (www.editage.com) for English language editing.

References

Angelim, M.K.S.C., de S. Maia, L.M.S., Mouffle, C., Ginhoux, F., Low, D., Amancio-Dos-Santos, A., Makhoul, J., Le Corronc, H., Mangin, J.M., Legendre, P., 2018. Embryonic macrophages and microglia ablation alter the development of dorsal root ganglion sensory neurons in mouse embryos. Glia 66, 2470–2486, http://dx.doi.org/10.1002/glia.23499.

Bennett, M.L., Bennett, F.C., Liddelow, S.A., Ajami, B., Zamanian, J.L., Fernhoff, N.B., Mulinyawe, S.B., Bohlen, C.J., Adil, A., Tucker, A., Weissman, I.L., Chang, E.F., Li, G., Grant, G.A., Hayden Gephart, M.G., Barres, B.A., 2016. New tools for studying microglia in the mouse and human CNS. Proc. Natl. Acad. Sci. U. S. A. 113, E1738–E1746, http://dx.doi.org/10.1073/pnas.1525528113.

Buch, T., Heppner, F.L., Tertilt, C., Heinen, T.J.A.J., Kremer, M., Wunderlich, F.T., Jung, S., Waisman, A., 2005. A Cre-inducible diphtheria toxin receptor mediates cell lineage ablation after toxin administration. Nat. Methods 2, 419–426, http://dx.doi.org/10.1038/nmeth762.

Buttgereit, A., Lelios, I., Yu, X., Vrohlings, M., Krakoski, N.R., Gautier, E.L., Nishinakamura, R., Becher, B., Greter, M., 2016. Sall1 is a transcriptional regulator defining microglia identity and function. Nat. Immunol. 17, 1397–1406, http://dx.doi.org/10.1038/ni.3585.

Cronk, J.C., Filiano, A.J., Louveau, A., Marin, I., Marsh, R., Ji, E., Goldman, D.H., Smirnov, I., Geraci, N., Acton, S., Overall, C.C., Kipnis, J., 2018. Peripherally derived macrophages can engraft the brain independent of irradiation and maintain an identity distinct from microglia. J. Exp. Med. 215, 1627–1647, http://dx.doi.org/10.1084/jem.20180247.

Cunningham, C.L., Martínez-Cerdeño, V., Noctor, S.C., 2013. Microglia regulate the number of neural precursor cells in the developing cerebral cortex. J. Neurosci. 33, 4216–4233, http://dx.doi.org/10.1523/JNEUROSCI.3441-12.2013.

Elmore, M.R.P., Najafi, A.R., Koike, M.A., Dagher, N.N., Spangenberg, E.E., Rice, R.A., Kitazawa, M., Matusow, B., Nguyen, H., West, B.L., Green, K.N., 2014. Colony-stimulating factor 1 receptor signaling is necessary for microglia viability, unmasking a microglia progenitor cell in the adult brain. Neuron 82, 380–397, http://dx.doi.org/10.1016/j.neuron.2014.02.040.

Erblich, B., Zhu, L., Etgen, A.M., Dobrenis, K., Pollard, J.W., 2011. Absence of colony stimulation factor-1 receptor results in loss of microglia, disrupted brain development and olfactory deficits. PLoS One 6, http://dx.doi.org/10.1371/journal.pone.0026317.

Galea, I., Palin, K., Newman, T.A., Van Rooijen, N., Perry, V.H., Boche, D., 2005. Mannose receptor expression specifically reveals perivascular macrophages in normal, injured, and diseased mouse brain. Glia 49, 375–384, http://dx.doi.org/10.1002/glia.20124.

Ginhoux, F., Guilliams, M., 2016. Tissue-resident macrophage ontogeny and homeostasis. Immunity 44, 439–449, http://dx.doi.org/10.1016/j.immuni.2016.02.024.

Ginhoux, F., Greter, M., Leboeuf, M., Nandi, S., See, P., Gokhan, S., Mehler, M.F., Conway, S.J., Ng, L.G., Stanley, E.R., Samokhvalov, I.M., Merad, M., 2010. Fate mapping analysis reveals that adult microglia derive from primitive macrophages. Science 330, 841–845.

Goldmann, T., Wieghofer, P., Jordão, M.J.C., Prutek, F., Hagemeyer, N., Frenzel, K., Amann, L., Staszewski, O., Kierdorf, K., Krueger, M., Locatelli, G., Hochgerner, H., Zeiser, R., Epelman, S., Geissmann, F., Priller, J., Rossi, F.M.V., Bechmann, I., Kerschensteiner, M., Linnarsson, S., Jung, S., Prinz, M., 2016. Origin, fate and dynamics of macrophages at central nervous system interfaces. Nat. Immunol. 17, 797–805, http://dx.doi.org/10.1038/ni.3423.

Han, J., Zhu, K., Zhang, X.M., Harris, R.A., 2019. Enforced microglial depletion and repopulation as a promising strategy for the treatment of neurological disorders. Glia 67, 217–231, http://dx.doi.org/10.1002/glia.23529.

Harrison, S.J., Nishinakamura, R., Jones, K.R., Monaghan, A.P., 2012. Sall1 regulates cortical neurogenesis and laminar fate specification in mice: Implications for neural abnormalities in Townes-Brocks syndrome. DMM Dis. Model. Mech. 5, 351–365, http://dx.doi.org/10.1242/dmm.002873.

Hattori, Y., Miyata, T., 2018. Microglia extensively survey the developing cortex via the CXCL12/CXCR4 system to help neural progenitors to acquire differentiated properties. Genes Cells 23, 915–922, http://dx.doi.org/10.1111/gtc.12632.
Hattori, Y., Naito, Y., Tsugawa, Y., Nonaka, S., Wake, H., Nagasawa, T., Kawaguchi, A., Miyata, T., 2020. Transient microglial absence assists postmigratory cortical neurons in proper differentiation. Nat. Commun. 11, http://dx.doi.org/10.1038/s41467-020-15409-3.
Hoeffel, G., Chen, J., Lavin, Y., Low, D., Almeida, F.F., See, P., Beaudin, A.E., Lum, J., Low, I., Forsberg, E.C., Poidinger, M., Zolezzi, F., Larbi, A., Ng, L.G., Chan, J.K.Y., Greter, M., Becher, B., Samokhvalov, I.M., Merad, M., Ginhoux, F., 2015. C-Myb+ erythro-myeloid progenitor-derived fetal monocytes give rise to adult tissue-resident macrophages. Immunity 42, 665–678, http://dx.doi.org/10.1016/j.immuni.2015.03.011.
Kaiser, T., Feng, G., 2019. Tmem119-EGFP and Tmem119-CreERT2 Transgenic Mice for Labeling and Manipulating Microglia, 6., pp. 1–18, http://dx.doi.org/10.1101/624825, bioRxiv.
Kierdorf, K., Erny, D., Goldmann, T., Sander, V., Schulz, C., Perdiguero, E.G., Wieghofer, P., Heinrich, A., Riemke, P., Hölscher, C., Müller, D.N., Luckow, B., Brocker, T., Debowski, K., Fritz, G., Opdenakker, G., Diefenbach, A., Biber, K., Heikenwalder, M., Geissmann, F., Rosenbauer, F., Prinz, M., 2013. Microglia emerge from erythromyeloid precursors via Pu.1-and Irf8-dependent pathways. Nat. Neurosci. 16, 273–280, http://dx.doi.org/10.1038/nn.3318.
Konishi, H., Kobayashi, M., Kunisawa, T., Imai, K., Sayo, A., Malissen, B., Crocker, P.R., Sato, K., Kiyama, H., 2017. Siglec-H is a microglia-specific marker that discriminates microglia from CNS-associated macrophages and CNS-infiltrating monocytes. Glia 65, 1927–1943, http://dx.doi.org/10.1002/glia.23204.
Konishi, H., Kiyama, H., Ueno, M., 2019. Dual functions of microglia in the formation and refinement of neural circuits during development. Int. J. Dev. Neurosci. 77, 18–25, http://dx.doi.org/10.1016/j.ijdevneu.2018.09.009.
Konishi, H., Okamoto, T., Hara, Y., Komine, O., Tamada, H., Maeda, M., Osako, F., Kobayashi, M., Nishiyama, A., Kataoka, Y., Takai, T., Udagawa, N., Jung, S., Ozato, K., Tamura, T., Tsuda, M., Yamanaka, K., Ogi, T., Sato, K., Kiyama, H., 2020. Astrocytic phagocytosis is a compensatory mechanism for microglial dysfunction. EMBO J. 39, 1–18, http://dx.doi.org/10.15252/embj.2020104464.
Lee, C.M., Zhou, L., Liu, J., Shi, J., Geng, Y., Liu, M., Wang, Jiaruo, Su, X., Barad, N., Wang, Junbang, Sun, Y.E., Lin, Q., 2020. Single-cell RNA-seq analysis revealed long-lasting adverse effects of tamoxifen on neurogenesis in prenatal and adult brains. Proc. Natl. Acad. Sci. U. S. A. 117, 19578–19589, http://dx.doi.org/10.1073/pnas.1918883117.
Lei, F., Cui, N., Zhou, C., Chodosh, J., Vavvas, D.G., Paschalis, E.I., 2020. CSF1R inhibition by a small-molecule inhibitor is not microglia specific; affecting hematopoiesis and the function of macrophages. Proc. Natl. Acad. Sci. U. S. A. 117, 23336–23338, http://dx.doi.org/10.1073/pnas.1922788117.
Malek, A., Sager, R., Schneider, H., 1998. Transport of proteins across the human placenta. Am. J. Reprod. Immunol. 40, 347–351, http://dx.doi.org/10.1111/j.1600-0897.1998.tb00064.x.
Marín-Teva, J.L., Dusart, I., Colin, C., Gervais, A., Van Rooijen, N., Mallat, M., 2004. Microglia promote the death of developing purkinje cells. Neuron 41, 535–547, http://dx.doi.org/10.1016/S0896-6273(04)00069-8.
Marsters, C.M., Nesan, D., Far, R., Klenin, N., Pittman, Q.J., Kurrasch, D.M., 2020. Embryonic microglia influence developing hypothalamic glial populations. J. Neuroinflammation 17, 1–17, http://dx.doi.org/10.1186/s12974-020-01811-7.
Masuda, T., Amann, L., Sankowski, R., Staszewski, O., Lenz, M., d'Errico, P., Snaidero, N., Costa Jordão, M.J., Böttcher, C., Kierdorf, K., Jung, S., Priller, J., Misgeld, T., Vlachos, A., Luehmann, M.M., Knobeloch, K.P., Prinz, M., 2020. Novel Hexb-based tools for studying microglia in the CNS. Nat. Immunol. 21, 802–815, http://dx.doi.org/10.1038/s41590-020-0707-4.
McKinsey, G.L., Lizama, C.O., Keown-Lang, A.E., Niu, A., Santander, N., Larpthaveesarp, A., Chee, E., Gonzalez, F.F., Arnold, T.D., 2020. A new genetic strategy for targeting microglia in development and disease. Elife 9, 1–34, http://dx.doi.org/10.7554/eLife.54590.
Mildner, A., Huang, H., Radke, J., Stenzel, W., Priller, J., 2017. P2Y12 receptor is expressed on human microglia under physiological conditions throughout development and is sensitive to neuroinflammatory diseases. Glia 65, 375–387, http://dx.doi.org/10.1002/glia.23097.
Miyamoto, A., Wake, H., Ishikawa, A.W., Eto, K., Shibata, K., Murakoshi, H., Koizumi, S., Moorhouse, A.J., Yoshimura, Y., Nabekura, J., 2016. Microglia contact induces synapse formation in developing somatosensory cortex. Nat. Commun. 7, http://dx.doi.org/10.1038/ncomms12540.
Munro, D.A.D., Bradford, B.M., Mariani, S.A., Hampton, D.W., Vink, C.S., Chandran, S., Hume, D.A., Pridans, C., Priller, J., 2020. CNS macrophages differentially rely on an intronic Csf1r enhancer for their development. Development 147, http://dx.doi.org/10.1242/dev.194449.
Paolicelli, R.C., Bolasco, G., Pagani, F., Maggi, L., Scianni, M., Panzanelli, P., Giustetto, M., Ferreira, T.A., Guiducci, E., Dumas, L., Ragozzino, D., Gross, C.T., 2011. Synaptic pruning by microglia is necessary for normal brain development. Science (80-.) 333, 1456–1458, http://dx.doi.org/10.1126/science.1202529.
Pont-Lezica, L., Beumer, W., Colasse, S., Drexhage, H., Versnel, M., Bessis, A., 2014. Microglia shape corpus callosum axon tract fasciculation: Functional impact of prenatal inflammation. Eur. J. Neurosci. 39, 1551–1557, http://dx.doi.org/10.1111/ejn.12508.
Prinz, M., Erny, D., Hagemeyer, N., 2017. Ontogeny and homeostasis of CNS myeloid cells. Nat. Immunol. 18, 385–392, http://dx.doi.org/10.1038/ni.3703.
Rigato, C., Buckinx, R., Le-Corronc, H., Rigo, J.M., Legendre, P., 2011. Pattern of invasion of the embryonic mouse spinal cord by microglial cells at the time of the onset of functional neuronal networks. Glia 59, 675–695, http://dx.doi.org/10.1002/glia.21140.
Rojo, R., Sauter, K.A., Lefevre, L., Hume, D.A., Pridans, C., bioRxiv 2018. Maternal Tamoxifen Treatment Expands the Macrophage Population of Early Mouse Embryos., pp. 296749, http://dx.doi.org/10.1101/296749.
Rosin, J.M., Vora, S.R., Kurrasch, D.M., 2018. Depletion of embryonic microglia using the CSF1R inhibitor PLX5622 has adverse sex-specific effects on mice, including accelerated weight gain, hyperactivity and anxiolytic-like behaviour. Brain Behav. Immun. 73, 682–697, http://dx.doi.org/10.1016/j.bbi.2018.07.023.
Saito, K., Okamoto, M., Watanabe, Y., Noguchi, N., Nagasaka, A., Nishina, Y., Shinoda, T., Sakakibara, A., Miyata, T., 2019. Dorsal-to-ventral cortical expansion is physically primed by ventral streaming of early embryonic preplate neurons. Cell Rep. 29 (1555–1567), e5, http://dx.doi.org/10.1016/j.celrep.2019.09.075.
Schafer, D.P., Lehrman, E.K., Kautzman, A.G., Koyama, R., Mardinly, A.R., Yamasaki, R., Ransohoff, R.M., Greenberg, M.E., Barres, B.A., Stevens, B., 2012. Microglia sculpt postnatal neural circuits in an activity and complement-dependent manner. Neuron 74, 691–705, http://dx.doi.org/10.1016/j.neuron.2012.03.026.
Silva, C.G., Peyre, E., Nguyen, L., 2019. Cell migration promotes dynamic cellular interactions to control cerebral cortex morphogenesis. Nat. Rev. Neurosci. 20, 318–329, http://dx.doi.org/10.1038/s41583-019-0148-y.
Squarzoni, P., Oller, G., Hoeffel, G., Pont-Lezica, L., Rostaing, P., Low, D., Bessis, A., Ginhoux, F., Garel, S., 2014. Microglia modulate wiring of the embryonic forebrain. Cell Rep. 8, 1271–1279, http://dx.doi.org/10.1016/j.celrep.2014.07.042.
Takagi, H., Fukaya, T., Eizumi, K., Sato, Y., Sato, Kaori, Shibazaki, A., Otsuka, H., Hijikata, A., Watanabe, T., Ohara, O., Kaisho, T., Malissen, B., Sato, Katsuaki, 2011. Plasmacytoid dendritic cells are crucial for the initiation of inflammation and t cell immunity in vivo. Immunity 35, 958–971, http://dx.doi.org/10.1016/j.immuni.2011.10.014.
Thion, M.S., Ginhoux, F., Garel, S., 2018. Microglia and early brain development: an intimate journey. Science (80-.) 362, 185–189, http://dx.doi.org/10.1126/science.aat0474.
Ueno, M., Fujita, Y., Tanaka, T., Nakamura, Y., Kikuta, J., Ishii, M., Yamashita, T., 2013. Layer v cortical neurons require microglial support for survival during postnatal development. Nat. Neurosci. 16, 543–551, http://dx.doi.org/10.1038/nn.3358.
Urbán, N., Guillemot, F., 2014. Neurogenesis in the embryonic and adult brain: same regulators, different roles. Front. Cell. Neurosci. 8, 1–19, http://dx.doi.org/10.3389/fncel.2014.00396.
Utz, S.G., See, P., Mildenberger, W., Thion, M.S., Silvin, A., Lutz, M., Ingelfinger, F., Rayan, N.A., Lelios, I., Buttgereit, A., Asano, K., Prabhakar, S., Garel, S., Becher, B., Ginhoux, F., Greter, M., 2020. Early fate defines microglia and non-parenchymal brain macrophage development. Cell 181 (557–573), e18, http://dx.doi.org/10.1016/j.cell.2020.03.021.
Van Hove, H., Martens, L., Scheyltjens, I., De Vlaminck, K., Pombo Antunes, A.R., De Prijck, S., Vandamme, N., De Schepper, S., Van Isterdael, G., Scott, C.L., Aerts, J., Berx, G., Boeckxstaens, G.E., Vandenbroucke, R.E., Vereecke, L., Moechars, D., Guilliams, M., Van Ginderachter, J.A., Saeys, Y., Movahedi, K., 2019. A single-cell atlas of mouse brain macrophages reveals unique transcriptional identities shaped by ontogeny and tissue environment. Nat. Neurosci. 22, 1021–1035, http://dx.doi.org/10.1038/s41593-019-0393-4.
Ved, N., Curran, A., Ashcroft, F.M., Sparrow, D.B., 2019. Tamoxifen administration in pregnant mice can be deleterious to both mother and embryo. Lab. Anim. 53, 630–633, http://dx.doi.org/10.1177/0023677219856918.
Voehringer, D., Liang, H.-E., Locksley, R.M., 2008. Homeostasis and effector function of lymphopenia-induced "Memory-Like" T cells in constitutively T cell-depleted mice. J. Immunol. 180, 4742–4753, http://dx.doi.org/10.4049/jimmunol.180.7.4742.
Wlodarczyk, A., Holtman, I.R., Krueger, M., Yogev, N., Bruttger, J., Khorooshi, R., Benmamar-Badel, A., Boer-Bergsma, J.J., Martin, N.A., Karram, K., Kramer, I., Boddeke, E.W., Waisman, A., Eggen, B.J., Owens, T., 2017. A novel microglial subset plays a key role in myelinogenesis in developing brain. EMBO J. 36, 3292–3308, http://dx.doi.org/10.15252/embj.201696056.
Yona, S., Kim, K.W., Wolf, Y., Mildner, A., Varol, D., Breker, M., Strauss-Ayali, D., Viukov, S., Guilliams, M., Misharin, A., Hume, D.A., Perlman, H., Malissen, B., Zelzer, E., Jung, S., 2013. Fate mapping reveals origins and dynamics of monocytes and tissue macrophages under homeostasis. Immunity 38, 79–91, http://dx.doi.org/10.1016/j.immuni.2012.12.001.
Zhang, J., Raper, A., Sugita, N., Hingorani, R., Salio, M., Palmowski, M.J., Cerundolo, V., Crocker, P.R., 2006. Characterization of Siglec-H as a novel endocytic receptor expressed on murine plasmacytoid dendritic cell precursors. Blood 107, 3600–3608, http://dx.doi.org/10.1182/blood-2005-09-3842.